



UNIVERSITY OF LEEDS

This is a repository copy of *The effect of vent size and congestion in large-scale vented natural gas/air explosions*.

White Rose Research Online URL for this paper:
<http://eprints.whiterose.ac.uk/85251/>

Version: Accepted Version

Article:

Tomlin, GB, Johnson, DM, Cronin, P et al. (2 more authors) (2015) The effect of vent size and congestion in large-scale vented natural gas/air explosions. *Journal of Loss Prevention in the Process Industries*, 35. 169 - 181. ISSN 0950-4230

<https://doi.org/10.1016/j.jlp.2015.04.014>

© 2015, Elsevier. Licensed under the Creative Commons Attribution-NonCommercial-NoDerivatives 4.0 International
<http://creativecommons.org/licenses/by-nc-nd/4.0/>

Reuse

Unless indicated otherwise, fulltext items are protected by copyright with all rights reserved. The copyright exception in section 29 of the Copyright, Designs and Patents Act 1988 allows the making of a single copy solely for the purpose of non-commercial research or private study within the limits of fair dealing. The publisher or other rights-holder may allow further reproduction and re-use of this version - refer to the White Rose Research Online record for this item. Where records identify the publisher as the copyright holder, users can verify any specific terms of use on the publisher's website.

Takedown

If you consider content in White Rose Research Online to be in breach of UK law, please notify us by emailing eprints@whiterose.ac.uk including the URL of the record and the reason for the withdrawal request.



eprints@whiterose.ac.uk
<https://eprints.whiterose.ac.uk/>

The Effect of Vent Size and Congestion in Large-Scale Vented Natural Gas/Air Explosions

Tomlin, G.^{1,2,*}, Johnson, D.M.², Cronin, P.², Phylaktou, H.N.¹, and Andrews, G.E.¹

¹ School of Chemical and Process Engineering, University of Leeds, Leeds, UK, LS2 9JT.

² DNV GL, Spadeadam Test Site, MoD R5, Gilsland, Brampton, Cumbria, UK, CA8 7AU,

*Corresponding author email: gary.tomlin@dnvgl.com

ABSTRACT

A typical building consists of a number of rooms; often with windows of different size and failure pressure and obstructions in the form of furniture and décor, separated by partition walls with interconnecting doorways. Consequently, the maximum pressure developed in a gas explosion would be dependent upon the individual characteristics of the building. In this research, a large-scale experimental programme has been undertaken at the DNV GL Spadeadam Test Site to determine the effects of vent size and congestion on vented gas explosions. Thirty-eight stoichiometric natural gas/air explosions were carried out in a 182 m³ explosion chamber of L/D = 2 and K_A = 1, 2, 4 and 9. Congestion was varied by placing a number of 180 mm diameter polyethylene pipes within the explosion chamber, providing a volume congestion between 0 and 5% and cross-sectional area blockages ranging between 0 and 40%. The series of tests produced peak explosion overpressures of between 70 mbar and 3.7 bar with corresponding maximum flame speeds in the range 35 - 395 m/s at a distance of 7 m from the ignition point. The experiments demonstrated that it is possible to generate overpressures greater than 200 mbar with volume blockages of as little as 0.57%, if there is not sufficient outflow through the inadvertent venting process. The size and failure pressure of potential vent openings, and the degree of congestion within a building, are key factors in whether or not a building will sustain structural damage following a gas explosion. Given that the average volume blockage in a room in a UK inhabited building is in the order of 17%, it is clear that without the use of large windows of low failure pressure, buildings will continue to be susceptible to significant structural damage during an accidental gas explosion.

KEYWORDS: congestion; gas explosion; obstacles; vented explosion.

1 INTRODUCTION

When a flammable gas/air mixture is ignited within a confined enclosure, there is an associated pressure rise. The pressure rise is caused by the restriction, that the enclosure places, on the expansion of the hot burnt gases. It is this rapid release of energy with its associated pressure generation and high temperature flame and gases that define a gas explosion. The level of damage a building sustains following a gas explosion is dependent upon the magnitude of the pressure generated and the relationship between the duration of the imposed pressure load and the natural period of vibration of the structure. Overpressures in the region of 30 -70 mbar have been shown to be capable of causing significant damage to industrial and residential buildings (Baker, Cox, Kulesz, Strehlow, & Westine, 1983). Other studies have shown (Astbury & Vaughan, 1972; Astbury, West, Hodgkinson, Cabbage, & Clare, 1970; Harris, 1983; West, Hodgkinson, & Webb, 1971a, 1971b; Wong & Karamanoglu, 1999) that an overpressure generated by a gas explosion, in the region of 200 mbar, has the potential to cause significant structural damage to buildings typically constructed in the UK.

In accidental vented confined explosions, the building is often vented, when a weak part of the structure fails (e.g. a window), and the pressure is relieved. Up until this point, the event may be considered as a confined explosion (with the potential to develop an overpressure of between 7 and 8 bar), but after venting begins, the rate of pressure rise, and hence the maximum pressure developed, is governed by the balance between the rate at which combustion products are produced and the rate of outflow through the venting process. The rate of outflow is dependent upon the size and location of the vent(s) (Alexiou, Andrews, & Phylaktou, 1997; Alexiou, Andrews, & Phylaktou, 1996; Alexiou, Phylaktou, & Andrews, 1996; Bauwens, Chaffee, & Dorofeev, 2010; Eckhoff, Fuhre, Guirao, & Lee, 1984; Fakandu, 2014; Fakandu, Andrews, & Phylaktou, 2014; Fakandu, Yan, Phylaktou, & Andrews, 2013; Mercx, van Wingerden, &

Pasman, 1993; Pappas, 1983; van Wingerden, 1989; van Wingerden & Zeeuwen, 1983c; Zalosh, 1980), whilst the rate at which hot combustion products are produced is directly related to the burning velocity of the fuel. Consequently, the rate of pressure rise in an accidental explosion is strongly dependent upon the fuels composition and on any turbulence that increases the burning velocity (and hence the flame speed).

Initially, after venting, unburnt gas/air mixture within the building will be expelled from the vent forming a flammable cloud outside the vent opening. When the burned gas reaches the vent opening, a sequence of interdependent events occur very quickly. Firstly, the volumetric flow of gas exiting the chamber increases, by a factor of approximately three, due to the decrease in density of the vented gas. This increase in venting causes a temporary reduction in the pressure within the enclosure as the rate of venting exceeds the volume expansion due to combustion and the inertia of the outflow 'over-vents' the burnt gases. Secondly, the pressure difference across the vent opening triggers a Helmholtz oscillation, which causes the internal chamber pressure to oscillate about the equilibrium pressure (Bauwens et al., 2010; Bauwens, Chaffee, & Dorofeev, 2009). Thirdly, the onset of burnt gas venting initiates Taylor instabilities, where the less dense burned gas is accelerated into the denser unburned gas/air mixture, increasing the mass combustion rate, and amplifying the Helmholtz oscillation. Finally, the venting flame front and the outflow of burnt gases ignite the flammable cloud outside the vent opening resulting in an external explosion. The explosion sends a propagating wave back towards the explosion chamber exacerbating the Taylor instabilities and causing the pressure inside the chamber to increase.

This complex sequence of events is further complicated if turbulence is generated by jet mixing in the gas/air mixture prior to ignition, or by induced flow interaction with obstacles. Both of these turbulence generating mechanisms may be important in accidental gas explosions in buildings;

the first, due to flow through interconnected rooms, and the second, due to the interaction of flow with furniture and décor. The enhanced combustion rate, caused by increases in the local transport of mass and energy, and increased flame surface area (Chan, Moen, & Lee, 1983) is dependent upon the induced flow velocity ahead of the flame, which itself is dependent upon the reaction rate. Consequently a ‘coupling’ is created which may manifest as a strong positive feedback mechanism (Schelkin mechanism) which, would result in continuous flame acceleration until the fuel is consumed, or transition to detonation occurs.

Previous studies have shown that reducing the vent size and increasing congestion, in the form of obstacles in the path of the propagating flame front, can affect flame speeds and result in increased overpressures in vented explosions (Alexiou, Phylaktou, et al., 1996; Bauwens et al., 2010; Bimson et al., 1993; Chan et al., 1983; Fakandu et al., 2013; Hall, Masri, Yaroshchik, & Ibrahim, 2009; Mercx et al., 1993; Na’inna, Phylaktou, & Andrews, 2013a, 2013b; Pappas, 1983; Park, Lee, & Green, 2008; Phylaktou & Andrews, 1994; Phylaktou, 1993; Pritchard, Hedley, & Webber, 2002; Solberg, Pappas, & Skramstad, 1980; Taylor & Bimson, 1989; van Wingerden, 1984a, 1984c; van Wingerden, 1989; van Wingerden & Zeeuwen, 1983a, 1983c; Zalosh, 1980, 2008).

Several studies (Harris & Wickens, 1989; Phylaktou, Alexiou, & Andrews, 1995; Phylaktou, 1993) have demonstrated that very fast flame speeds, in excess of 600 m/s, may be generated when a flame propagates through a flammable gas/air mixture in the presence of repeated obstacles. To predict the pressure generated during these type of fast flame events, it is necessary to understand the role that the obstacle configuration, blockage ratio, and the parameters that affect the turbulent flow field, play in effecting the strength of the feedback mechanism.

Whilst the identified studies have demonstrated that reducing the vent size and increasing congestion can affect the flame speed and increase overpressures, the confined and congested situation found in buildings, wherein both adiabatic expansion and turbulent flame acceleration play a role, has received little large-scale attention. Typical industrial buildings or dwellings will have a pathway, for flame propagation, that consists of a number of interconnected rooms, each of which may have significant congestion. For example, in the average UK home a doorway represents an opening with a blockage of approximately 82% and the average room congestion is approximately 17% (Admirals Storage; BBC news, 2011; Drury, Watson, Broomfield, Levitt, & Tetlow, 2006). Inadvertent individual vent openings, in the form of windows, will provide a minimum area vent coefficient (K_A), defined as the area of the front face of the chamber divided by the area of the vent opening ($K_A = A/A_v$) (Harris, 1983)¹, of 4 where openings are provided on one wall of the room or 8 if windows are

¹ The vent coefficient may be expressed in other terms (e.g. $K = A_{cs}/A_v$ or $K_v = V^{2/3}/A_v$) but in the context of this work (i.e. adventitious vent openings), K_A was chosen as being most appropriate. However, the experimental data is currently being analysed with reference to explosion relief design standards and this will be the subject of a further paper.

provided on more than one wall (Greater London Authority, 2012). To understand the effects of window size and obstacles, in the development of explosions in buildings, a large-scale experimental programme was undertaken at the DNV GL Spadeadam Test Site. Some of the results of this programme are presented in this paper.

2 THE EXPERIMENTAL PROGRAMME

In total, thirty-eight large-scale vented confined explosion experiments were carried out at the Spadeadam Test Site using stoichiometric natural gas/air mixtures in a 182 m³ steel explosion chamber of $L/D = 2$ (Fig. 1). The explosion chamber, of dimensions 9.0 m x 4.5 m x 4.5 m, was constructed of 10 mm thick steel plates supported by regularly spaced I beams. The rear face of the chamber was constructed of two hinged pressure relief panels, with a failure overpressure of 4 bar, to protect the explosion chamber from damage during the experiments. The front face of the chamber accommodated a vent opening of variable size which was covered by a polythene sheet (low failure pressure) to prevent the gas/air mixture escaping during filling. The vent openings were either 20.25 m², 10.13 m², 5.06 m² or 2.25 m². Correspondingly, the vent coefficients (K_A), were approximately 1, 2, 4 or 9.



Fig. 1. The explosion chamber.

Obstacle supports were attached to the side walls of the explosion chamber such that eight pipe arrays, each capable of supporting up to ten horizontal pipes, of 4.5 m in length and 0.18 m in diameter, could be positioned perpendicular to the direction of flame propagation. The array supports were positioned at 1 m intervals along the length of the explosion chamber, with the 1st array positioned 1 m from the rear wall. This meant that a maximum of 80 x 180 mm diameter pipes could be positioned within the chamber providing a maximum area blockage (AB) of approximately 40% and a maximum volume blockage (VB) of approximately 5%. The area blockage was calculated as the percentage of the cross-sectional area of the explosion chamber occupied by the pipes in a single array. The volume blockage was calculated as the percentage of the total volume of the chamber occupied by the pipes in all arrays. The number of obstacles and the distance between obstacles was varied during the experiments so the effects of volume blockage and obstacle separation distance on flame speed and overpressure could be investigated. The types of obstacle arrangement used in the experiments are shown in Fig. 2.

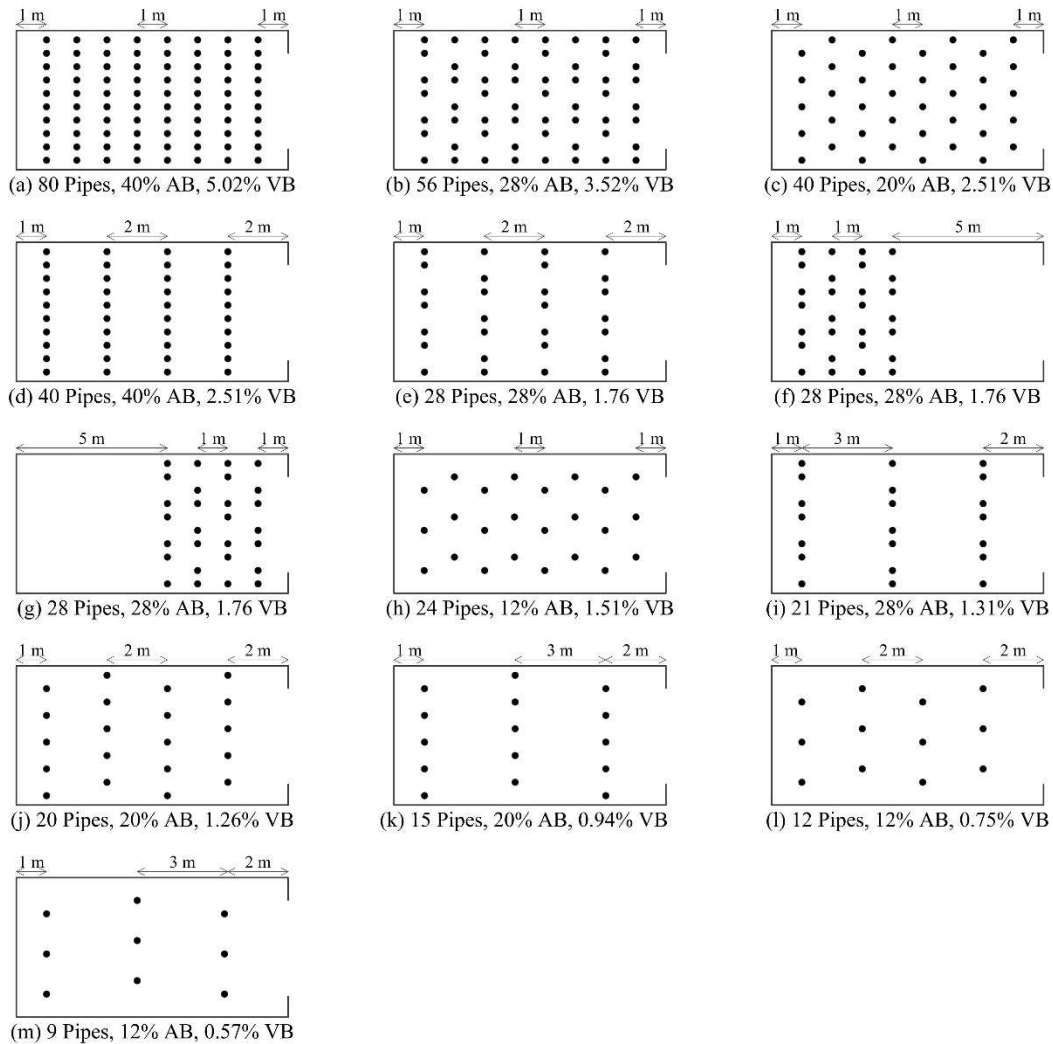


Fig. 2. Obstacle type and configuration.

The required natural gas/air mixtures were obtained by ‘purge- filling’ the rig. Natural gas was provided from the Spadeadam high pressure gas reservoir and passed through a local pressure reducing station to reduce the pressure from 200 bar to 1 - 3 bar before being admitted to the filling system. A polythene tube was used to mix the gas with air. The polythene tube was connected at one end to an opening at the bottom of the explosion chamber and at the other end to the gas supply and to an air supply from a motor driven fan. Gas was released into the tube via a valve controlled by a Supervisory Control and Data Acquisition (SCADA) system and air was blown into the tube via a 5.7 kW axial fan. The volume flow rate of air was controlled by varying the fan speed using the SCADA system and the gas flow rate was controlled by altering the gas valve position. Once the required gas/air concentration had been reached in the chamber, the gas supply to the chamber was isolated, the air fan switched off and the mixture was allowed to become quiescent. The gas concentration was measured using an infrared analyser and flame ionization detector. Three fuel gas sample lines to the analysers were used to determine the gas concentration within the chamber; one at high level, one at low level and one close to the point of ignition. This filling method was found to produce homogenous mixtures with no significant difference in measurements across sample points.

The natural gas/air mixture was ignited by a single, low energy, electric spark (3 mm spark gap) located in the centre

of the rear wall of the explosion chamber. The spark was generated through the discharge of a 68 μF capacitor, charged to 160 Vdc through the primary windings of a high tension coil. The pressure generated in the explosion was measured using eight piezoelectric pressure transducers located at strategic positions both inside and outside the explosion chamber (Table 1). The pressure transducers located within the explosion chamber were secured to the floor whilst the transducers outside the chamber were mounted on stands (positioned perpendicular to the vent opening to measure side-on overpressure) approximately 1.5 m above ground level. The time of flame arrival, was measured using ten flame ionisation probes located along the centre line of the chamber (Table 1), with voltage outputs being registered on the SCADA system. The flame speed was calculated using the measured flame arrival times. The explosions were also filmed using high speed video (400 frames per second).

Table 1. Location of pressure transducers and flame ionisation probes.

Pressure transducer			Flame ionisation probe	
No.	Location	Distance from rear wall (m)	No.	Distance from rear wall (m)
T1		0.4	I1	0.900
T2	Inside explosion chamber	3.5	I2	3.375
T3		6.5	I3	3.625
T4		7.5	I4	6.375
T5		8.5	I5	6.625
T6	Outside explosion chamber	13	I6	7.375
T7		17	I7	7.625
T8		45	I8	8.250
			I9	8.500
		I10	8.750	

3 TEST CONDITIONS

A summary of the experimental test conditions and data gathered from the thirty-eight explosion tests is contained in Table 2, in terms of overpressures and maximum flame speeds. The main variables of interest in this study were vent size (i.e. representative of differing window sizes in buildings) and degree of congestion within the explosion chamber.

Table 2. Summary of test conditions and experimental data.

Test No.	Vent Coeff.		Congestion		P_V^2 (mbar)	P_b^2 (mbar)	P_{ext}^2 (mbar)	P_{mfa}^2 (mbar)	P_{max}^2 (mbar)	Flame Speed ³ (m/s)
	K_A	Type	AB (%)	VB (%)						
1	1	-	0.0	0.00	14	22	69	44	69	35
2	1	m	12.0	0.57	14	81	155	120	155	88
3	1	l	12.0	0.75	14	112	135	157	157	86
4	1	k	20.0	0.94	14	108	145	119	145	83
5	1	j	20.0	1.26	11	203	246	-	246	89
6	1	l	28.0	1.31	13	365	380	368	380	145
7	1	h	12.0	1.51	13	309	336	285	336	152
8	1	e	28.0	1.76	11	374	393	418	418	149
9	1	c	20.0	2.51	20	547	713	715	715	192
10	1	d	40.0	2.51	20	-	903	815	903	210
11	1	b	28.0	3.52	21	1350	1425	1296	1425	262
12	1	a	40.0	5.02	18	2793	2992	2272	2992	395
13	1	a	40.0	5.02	-	3367	3474	2941	3474	-
14	2	-	0.0	0.00	12	23	92	-	92	143
15	2	m	12.0	0.57	14	301	477	671	671	86
16	2	l	12.0	0.75	20	320	677	405	677	102
17	2	j	20.0	1.26	21	555	1079	790	1079	111
18	2	h	12.0	1.51	18	-	719	1036	1036	109
19	2	f	28.0	1.76	20	686	678	1614	1614	125
20	2	e	28.0	1.76	15	661	780	1281	1281	109
21	2	g	28.0	1.76	-	691	1073	969	1073	66
22	2	c	20.0	2.51	17	1162	1259	1937	1937	172
23	2	d	40.0	2.51	-	1641	1934	1979	1979	176
24	2	b	28.0	3.52		1801	1986	2273	2273	185
25	4	-	0.0	0.00	20	96	183	132	183	132
26	4	l	12.0	0.75	-	-	-	1058 ⁴	1058	103
27	4	j	20.0	1.26	-	-	-	1397 ⁴	1397	114
28	4	c	20.0	2.51	-	1293	-	2152 ⁴	2152	115
29	4	b	28.0	3.52	-	2185	2508	2992	2992	203
30	9	-	0.0	0.00	26	-	-	353 ⁴	353	417
31	9	l	12.0	0.75	-	-	-	1598 ⁴	1598	64
32	9	k	20.0	0.94	-	1406	-	2006 ⁴	2006	72

² Measurement taken from a piezoelectric pressure transducer located 0.4 m from the spark igniter

³ Flame speed calculated at a distance 7.5 m from the spark igniter

⁴ Relatively long duration peak, combination of P_{ext} and P_{mfa}

Test No.	Vent Coeff.		Congestion		P_V^2 (mbar)	P_b^2 (mbar)	P_{ext}^2 (mbar)	P_{mfa}^2 (mbar)	P_{max}^2 (mbar)	Flame Speed ³ (m/s)
	K_A	Type	AB (%)	VB (%)						
33	9	j	20.0	1.26	-	-	-	2134 ⁴	2134	88
34	9	j	20.0	1.26	-	-	-	2262 ⁴	2262	-
35	9	j	20.0	1.26	-	-	-	2162 ⁴	2162	-
36	9	h	12.0	1.51	-	-	-	2098 ⁴	2098	70
37	9	c	20.0	2.51	-	-	-	2996 ⁴	2996	-
38	9	b	28.0	3.52	-	-	-	3700 ⁴	3700	-

4 RESULTS AND DISCUSSION

4.1 General Remarks

Vented explosions typically exhibit a series of pressure peaks; of which, not all are present in all explosions, and which have been interpreted in a number of different ways (Bauwens et al., 2010; Bimson et al., 1993; Cooper, Fairweather, & Tite, 1986; Fakandu, Kasmani, Andrews, & Phylaktou, 2011; Fakandu et al., 2013; Harrison & Eyre, 1987; Mercx et al., 1993; Pappas, Solberg, & Foyn, 1984; van Wingerden, 1984a; van Wingerden, 1989; Zalosh, 1980). For clarity, in this study, the following definitions are used to describe the pressure peaks; P_V is used to label the pressure peak associated with the opening of the vent, P_b is used to label the peak associated with the onset of burnt gas venting, P_{ext} is used to label the peak associated with the external explosion and P_{mfa} is used to label the peak associated with the maximum flame area or maximum flame speed. Pressure peaks associated with oscillatory combustion or acoustic effects have not been considered in this study.

The pressure transducers used during this study were not separated equidistantly and different overpressure-time profiles were recorded. The maximum pressure was consistently measured at the rear of the explosion chamber (transducer T1) and for consistency, this is the value that is reported in the results. In Fig. 3, a pressure-time profile is shown for an explosion in an empty enclosure with a vent size of $K_A = 1$; four distinct pressure peaks are evident.

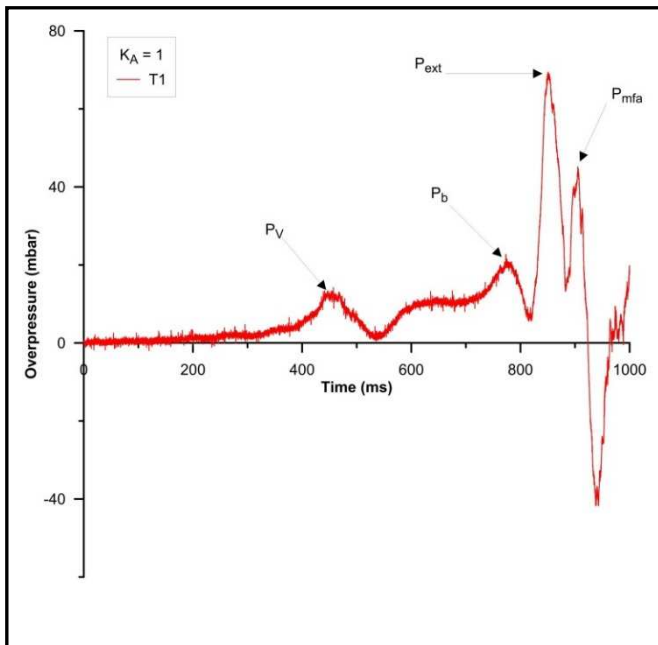


Fig. 3. Pressure-time profile for test number 1.

The first pressure peak, P_V , corresponds to the failure of the polythene sheet at a time of around 450 ms after ignition. The polythene sheet failed at an overpressure of approximately 14 mbar and as this does not represent a significant pressure gradient across the vent opening, the rate of unburnt gas/air outflow is relatively low. The second pressure peak, P_b , corresponds to the onset of burnt gas venting at a time of approximately 775 ms and was recorded as the time that the flame front reached the plane of the vent opening. With the onset of burnt gas venting, the volumetric outflow rate increases dramatically as the volumetric flow through the vent is inversely proportional to the square root of the density of the gas being vented. This significant increase in outflow manifests itself as a drop in pressure on the pressure-time profile resulting in the pressure peak P_b . The third pressure peak corresponds to the external explosion, which occurs when the previously vented unburnt gas/air mixture is ignited by the flame front when it exits the vent opening.

In Fig. 4, a pressure-time profile, recorded on pressure transducers T1 and T6, is shown for test number 2. Transducer T1 was located 0.4 m from the rear of the explosion chamber and transducer T6 was located 4 m outside the vent opening resulting in a distance of 12 m between the transducers. The speed of sound in the combustion products of a stoichiometric methane/air was calculated to be 992 m/s meaning that if the pressure wave generated by the external explosion was propagating into the explosion chamber, giving rise to a pressure peak, P_{ext} , it would be recorded at transducer T1, 12 ms after it was recorded at T6.

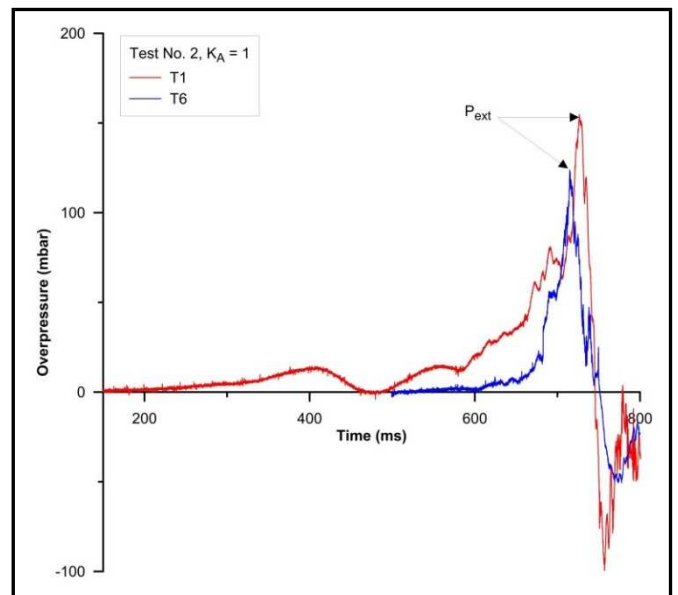


Fig. 4. Pressure-time profile showing the effects of the external explosion.

In Fig. 4 it can be seen that the external explosion was recorded on T6 at 715 ms, generating a pressure peak of 123 mbar. The corresponding pressure peak on T1, identical in its profile but of greater magnitude, was recorded at 727 ms and generated a pressure peak of 155 mbar. Importantly, in all but two of the experiments (test no's 3 and 5, where the pressure peak was of the same magnitude), the magnitude of the pressure inside the enclosure was greater than that recorded outside. Consequently, the external combustion event cannot be solely attributable to the pressure peak generated within the explosion chamber, and whilst it was evident that the pressure peak was triggered by the external explosion, its magnitude was caused by a combination of the propagation of the external pressure wave into the enclosure, the temporary restriction to the outflow of gases caused by the reduced pressure differential across the vent opening following the external combustion, and by increases in the rate of combustion caused by turbulence and Taylor instabilities. In Fig. 3, the fourth pressure peak corresponds to the time at which the flame surface area was at its greatest, giving rise to the pressure peak, P_{mfa} . This peak was seen on a number of tests to be superimposed onto the P_{ext} pressure peak.

Taylor instabilities are hydrodynamic instabilities introduced when the less dense burned gases are accelerated into the denser unburned gas/air mixture, thereby creating a large increase in flame surface area. Taylor instabilities are most commonly observed with central ignition and are a contributor to the low frequency oscillatory combustion frequently observed with vented explosions (Bauwens et al., 2010; Bauwens et al., 2009). During the early stage of burnt gas venting, the flame front is accelerated outside of the enclosure creating a 'pear' shaped flame front (in the case of central ignition). When the flame front is accelerated in this direction, the Taylor effect stabilises the rear of the flame front, inside the enclosure, resulting in a reduced mass combustion rate, causing a fall in pressure. This fall in pressure triggers an acceleration of the flame front in the opposite, Taylor unstable direction, thereby increasing the flame surface area and causing a pressure rise in the enclosure. This low frequency oscillatory combustion may continue until all the fuel is consumed. A similar effect may be observed with rear ignition, where, following the external explosion, Taylor instabilities are introduced as the burned gases are accelerated into the unburned gas/air mixture trapped in the corners of the explosion chamber.

Although the type of pressure-time profile shown in Fig. 3 was exhibited on a significant number of the explosion tests, there were a number of experiments where the maximum pressure peak was of longer duration than that seen in Fig. 3 (caused by a combination of the P_b , P_{ext} , and P_{mfa} pressure peaks) and the P_V and P_b pressure peaks were not obvious as a consequence of the magnitude of the maximum pressure peak.

The series of tests produced peak explosion overpressures of between 70 mbar ($K_A = 1$ and no congestion) to 3.7 bar ($K_A = 9$ and 3.52% VB) with corresponding maximum flame speeds in the range 35 - 395 m/s at a distance of 7 m from the ignition point. Flame speeds in excess of 600 m/s were consistently recorded close to the vent opening during tests with area blockages of 20% or greater combined with a volume blockage greater than 1.5%. One test configuration (Type a), was only utilised for tests with a vent opening of

$K_A = 1$, as the overpressures predicted for tests involving a vent opening of $K_A = 2, 4$ or 9, based on earlier experiments, exceeded the design strength of the explosion chamber.

Whilst the results of these tests show that high and damaging overpressures can be generated even from relatively benign confined explosions in empty (no internal congestion) chambers with large vent areas, the presence of congestion can significantly increase the overpressures generated, often by more than an order of magnitude. The significance of these results is that they confirm that the size of the vent opening and the degree of congestion within a building are key factors in whether or not a building will sustain structural damage following a gas explosion. The experiments demonstrated that it is possible to generate overpressures greater than 200 mbar with volume blockages of as little as 0.57%, if vent openings do not allow sufficient outflow.

It is recognised that the effect of area blockage and obstacle array separation distance may play a more important role in the development of fast flames than volume blockage. However, whilst chemical, process and storage facilities, will have congested region layouts or designs that are readily available, populated buildings will have congested and confined areas that are not predictable, and, as a consequence, it was considered appropriate to use volume blockage as the main criteria for the study. Consequently, volume blockage was the main variable considered during the design of the congestion configuration. The results of this work have been compared with tests conducted with furniture as part of an extended study and will be published in another paper.

4.2 Effect of Vent Size

4.2.1 Effect on Overpressure

In Fig. 5, the effect of vent size (i.e. confinement) on overpressure is shown for explosions with no congestion. It can be seen that the overpressure and the duration of the maximum pressure peak increases as the vent size is reduced. Furthermore, the maximum pressure peak on the $K_A = 9$ pressure-time profile is significantly longer in duration, has a shallower gradient than tests with larger vent openings and also exhibits a number of oscillatory peaks. These observations are attributed to the influence of turbulence and Taylor instabilities caused by the significant amount of unburnt gas that gets 'trapped' in the corners of the explosion chamber.

It was also noted that as the vent size was increased, the magnitude of P_b decreased because unburnt gas venting was not significantly restricted by the vent opening and the external explosion, P_{ext} , was dominant. However, as the size of the vent was reduced, the outflow through the vent was restricted, which increased the magnitude of P_b , and the external explosion became less significant, and in some instances, typically with $K_A = 9$, resulted in its pressure peak, P_{ext} merging with the pressure peak P_b , to produce a single broad peak (sometimes also merging with P_{mfa}). It was also evident that it triggered Taylor instabilities.

The effect of vent size on empty enclosures with regard to maximum overpressures was also very interesting. The magnitude of the $K_A = 9$ maximum overpressure was found to be twice that of the corresponding value for $K_A = 4$, four times that of $K_A = 2$ and five times that of $K_A = 1$.

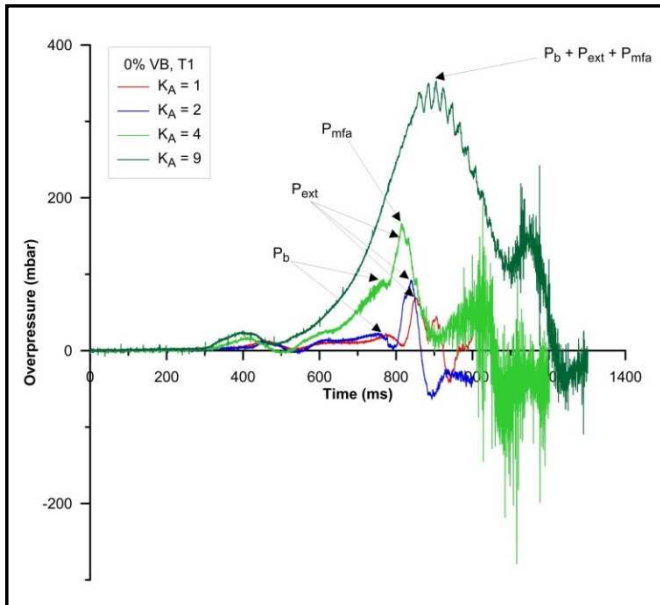


Fig. 5. The effect of vent size on overpressure (no congestion).

In Fig. 6, the effect of vent size on overpressure is shown for tests where congestion was present in the enclosure. It can be seen that as the vent size was decreased, the magnitude of the maximum pressure peak increased. In a similar manner to tests without congestion, the influence of the external explosion, on the pressure generated within the enclosure, reduced with decreasing vent size and increasing congestion, with the pressure peak P_{ext} , merging with the pressure peaks P_b and P_{mfa} to produce a single broad peak. Furthermore, the average rate of pressure rise, $(dP/dt)_{avg}$, from the onset of the maximum pressure peak, ranged from 2.8 bar/s for $K_A = 1$, to 17.4 bar/s for $K_A = 9$ indicating that there is a direct correlation between both the rate of pressure rise and maximum overpressure with reducing vent size.

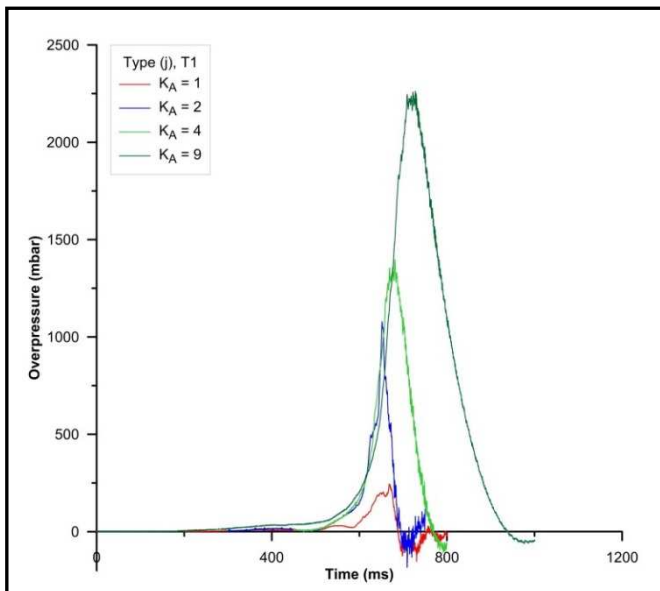


Fig. 6. The effect of vent size on overpressure (type (j) congestion).

It was observed that in tests conducted with a larger vent size (i.e. $K_A = 1$), the flame typically emerged from the vent as a narrow jet and a few metres from the plane of the vent opening, the jetting flame front ignited the unburnt gas/air mixture and flame propagated rapidly in a 'mushroom' shape, giving rise to the peak external overpressure. As the vent size

was decreased, the pressure at which flame venting occurred increased and as a consequence the emerging jet velocity increased and the unburnt gas/air mixture was distributed farther from the vent opening. In addition, the time taken for flame venting increased as the vent area was decreased, allowing more time for the vented gases to travel farther from the vent opening. In these instances, the external flame propagation did not appear mushroom shaped, but rather, was elongated, with the centre of the external explosion typically being several metres from the plane of the vent opening. For this reason, and because the smaller vent opening limits the size of the pressure wave that can propagate back into the enclosure, the influence of the external explosion was observed to be greater with larger vent openings.

The effect of vent size on the pressure generated outside the explosion chamber is shown in Fig. 7. This diagram shows the maximum overpressure recorded, as a consequence of the external explosion, by the transducers located outside the explosion chamber. The results show that decreasing the size of the vent gives rise to an increase in external overpressures. This increase in pressure is a result of the small vent area causing flammable unburnt gas/air mixture ahead of the flame front to be vented at far higher velocities than is the case for larger vent areas. This high efflux velocity causes greater turbulence within the external flammable gas cloud, which causes faster burning velocities (and hence flame speeds) and higher external overpressures, though of shorter duration. The plot also highlights the effect of decreasing vent size discussed above, with the $K_A = 9$ tests with congestion registering a greater overpressure at the T7 location than at T6.

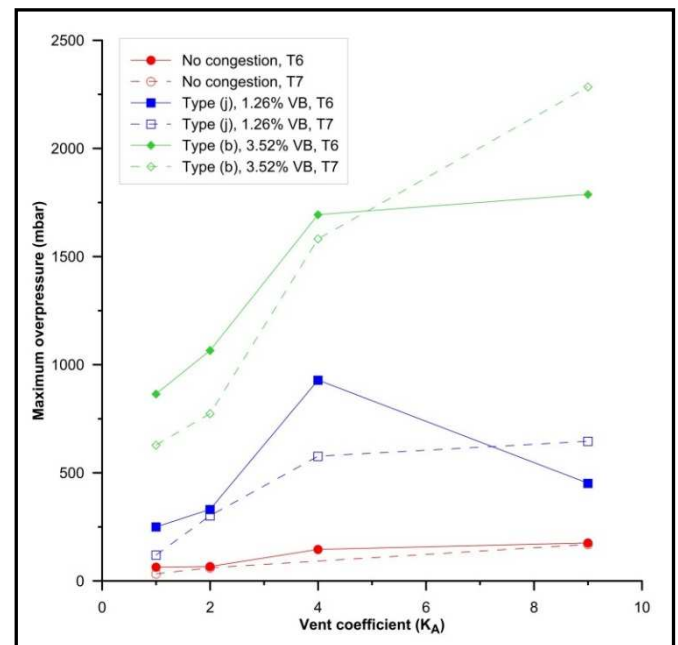


Fig. 7. The effect of vent size on external pressure.

4.2.2 Effect on Flame Speed

In Fig. 8, the effect of vent size on flame speed is shown for explosions with no congestion. As the flame speed is a combination of the rate of combustion and the induced flow velocity, a change in either alters its magnitude. However, the two properties are not independent, as combustion generates pressure, and pressure generates flow (Schelkin Mechanism). The 'induced' flow, in terms of turbulent vented explosions,

is typically of the order of 80 – 85% of the flame speed (Harris & Wickens, 1989), and consequently, any change in outflow velocity will significantly affect the flame speed. As seen in Fig. 8, reducing the vent size resulted in increased flame speeds as the flame approaches the vent, suggesting that for explosions without congestion, there is an indirect

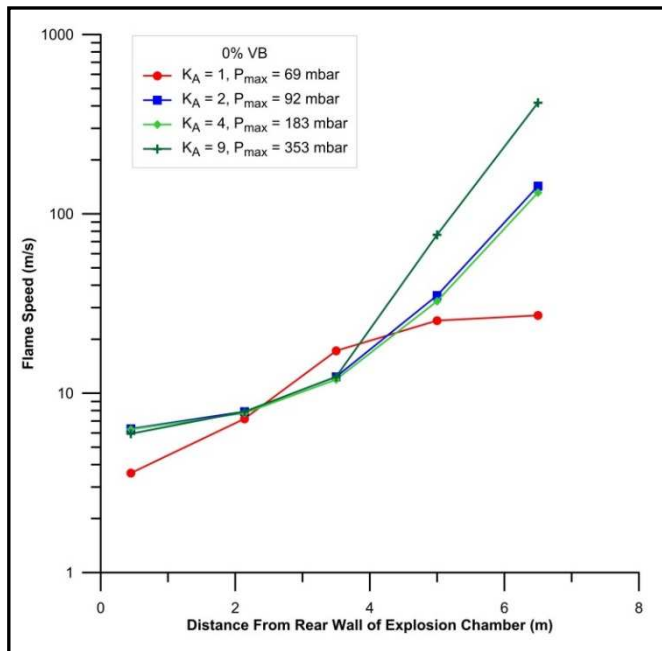


Fig. 8. The effect of vent size on flame speed (no congestion).

The effect of varying the vent size where congestion is present in the enclosure is shown in Fig. 9 and Fig. 10. In Fig. 9, the calculated flame speed, taken from the flame arrival times, for tests with 0.75 % volume blockage is shown and Fig. 10 plots the calculated flame speeds for tests with 1.26% volume blockage. It can be seen in Fig. 9 that in the early stages of the explosions (flame travel ≤ 5 m), the flame speeds are significantly faster than those tests where no congestion was present, and that, unlike the results shown in Fig. 8, reducing the vent size resulted in reduced flame speeds. However, as the flame approached the vent opening, the flame speeds increased rapidly and increased with reduced vent size. The flame speeds were found to decrease as the vent size was reduced (Fig. 10); an effect that was most significant when the volume blockage was greater than 2%, with the fastest flame speeds being generated in the $K_A = 1$ tests. Reducing the vent opening (i.e. increasing confinement) tended to reduce the speeds of the flowing mixture inside the chamber, except in regions close to the opening, which reduces the flame speed. In certain instances, choked flow conditions occurred. Choked flow occurs in vented explosions when the unburnt gas/air mixture and/or burnt gases passing through the vent opening are initially subsonic (upstream of the vent opening), and the principles of the conservation of mass require the fluid to increase in velocity as it flows through the reduced cross-sectional area of the vent opening. This increase in velocity will continue until the limiting conditions of choked flow are reached. This limiting condition occurs when the fluid approaches the local speed of sound (i.e. Mach number 1) and consequently the velocity cannot be increased by increasing the upstream pressure or reducing the downstream pressure. However, the mass flow rate may be increased by increasing the upstream pressure, which will increase the density of the fluid across the vent opening, but will not increase its velocity. The onset of

correlation between flame speed and vent size. It should be noted that the flame speeds are measured along the centreline and that reducing the vent size increases the internal pressure giving rise to greater flow velocities. This has the effect of producing greater distortion of the flame, particularly along the centreline.

choked flow may be estimated in vented natural gas/air explosions as the condition occurs when the critical pressure ratio, that is the ratio of the absolute pressure immediately upstream of the vent opening to the absolute pressure immediately downstream of the vent opening is approximately 1.89 for the unburnt gas/air mixture and 1.80 for the burnt gases under stoichiometric conditions. Consequently, choked flow conditions cannot occur at overpressures, within the enclosure, less than 900 mbar.

It may be concluded therefore, that reducing the vent size, for a given level of congestion, results in increased flame speeds up until the point where the fluid velocity through the vent opening reaches the local speed of sound. After this point, reducing the vent opening results in the flame speed being reduced, except in the region of the vent opening. In addition, the reduction in flow velocity will result in comparatively lower levels of turbulence in the wake of obstacles and this will result in less enhancement of combustion rates and hence comparatively low flame speeds.

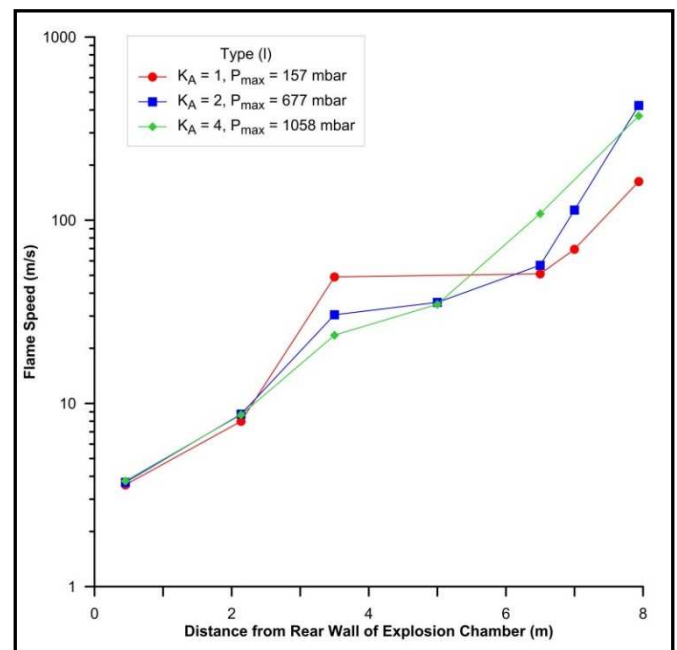


Fig. 9. The effect of vent size on flame speed (type (I) congestion).

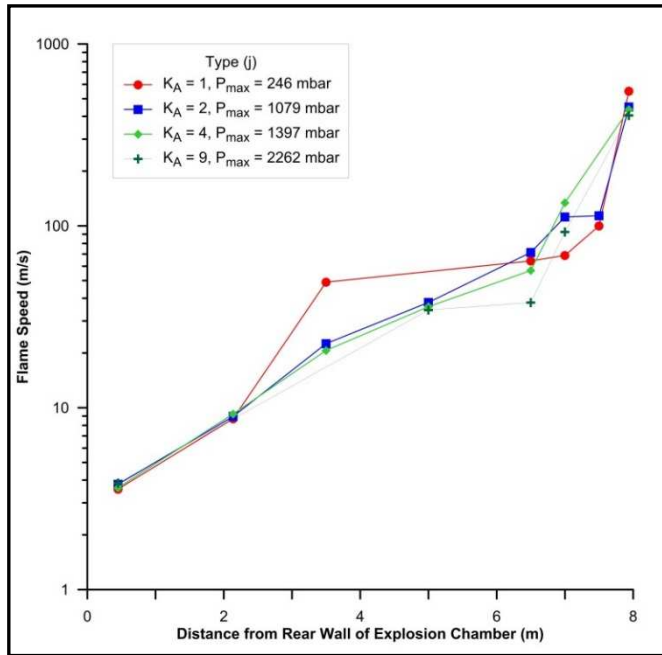


Fig. 10. The effect of vent size on flame speed (type (j) congestion).

4.3 Effect of Congestion

Congestion increases the flame speed, and consequently, the overpressure as a result of three mechanisms. Firstly, the flame surface area increases due to the distortion of the flame as it flows around the obstacles that form the congested region. This leads to an increase in the overall mass burning rate, thereby increasing the flame speed. Secondly, the unburnt mixture being pushed ahead of the flame will create turbulence in the wake of the obstruction. Thirdly, when the flame front reaches this turbulent region there is an increase in the rate of heat and mass transfer within the reaction zone, the burning velocity is therefore enhanced and this also increases the flame speed, setting up the positive feedback process. This results in the faster production of combustion products, which further enhances the flow and initiates a change from laminar to turbulent conditions. The first mechanism was found to be more significant in the early stages of the explosion process when the flame front is moving relatively slowly and few turbulence generating obstacles have been encountered. By contrast, the second mechanism will be more significant when the flame speed is already high as the higher flow speeds cause increased levels of turbulence to be created in the wake of obstacles. Therefore turbulence will be more significant later in the explosion process when the flame will have progressed farther along the enclosure.

4.3.1 Effect of Volume Blockage

A pressure-time profile for an explosion involving a type (j) obstacle configuration with a vent size of $K_A = 1$ is shown in Fig. 11. This configuration consisted of four arrays, each containing five pipes. The first array was located 1 m from the rear of the enclosure and the pitch between arrays was set at 2 m. The times at which the flame front arrived at the obstacle arrays have been plotted on the graph so that the effects of obstacles on overpressure may be observed; three distinct pressure peaks are evident.

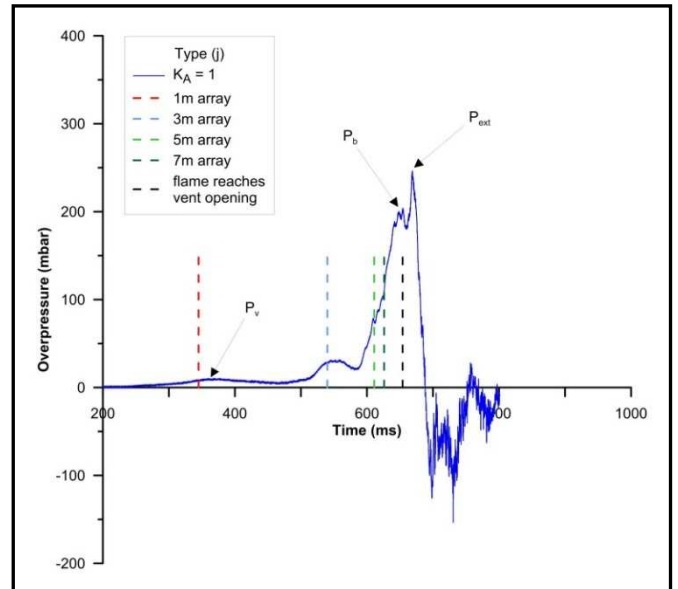


Fig. 11. Pressure-time profile for type (j) explosion, $K_A = 1$.

The first pressure peak occurs approximately 360 ms after ignition and corresponds to the flame passing through the 1st obstacle array but also may be associated with the failure of the polythene sheet. This peak occurs at an overpressure of approximately 14 mbar, and as this does not represent a significant pressure gradient across the vent opening, the rate of unburnt gas/air outflow is relatively low and the pressure peak is not significant. The second pressure peak occurs at approximately 560 ms and corresponds to the flame arrival at the second pipe array (located at 3 m). At this point the flame speed was in the order of 50 m/s but with the downstream obstacle array 2 m away, the enhanced combustion in the wake of the second array did not extend the full gap between the arrays and the flame speed started to decrease, resulting in the pressure falling, giving the second pressure peak. The influence of the 5 m and 7 m obstacle arrays are evident as changes in the gradient of the pressure-time curve, indicating that the flame speed is increasing. The third pressure peak, P_b , corresponds to the onset of burnt gas venting at a time of approximately 680 ms. The fourth pressure peak corresponds to the external explosion, which occurs when the previously vented unburnt gas/air mixture is ignited by the flame front when it exits the vent opening.

A pressure-time profile for an explosion involving a type (a) obstacle configuration with a vent size of $K_A = 1$ is shown in Fig. 12. This configuration consisted of eight arrays, each containing ten pipes and was the most congested set-up that was used in the experimental programme. It was only used on the largest vent size in order to prevent damage to the explosion chamber. The first array was located 1 m from the rear of the enclosure and the pitch between arrays was set at 1 m. The time at which the flame front arrived at the first seven of the eight obstacle arrays is plotted on the graph so the effects of congestion on overpressure can be observed. It was not possible to plot the flame arrival at the final array as the ionisation probe triggered early, possibly due to the high flow speeds. The flame speed in the region of the vent opening however, was in excess of 600 m/s. The effect of the 1st obstacle array is not immediately obvious on the pressure time profile but it is important as it has established flow within the chamber.

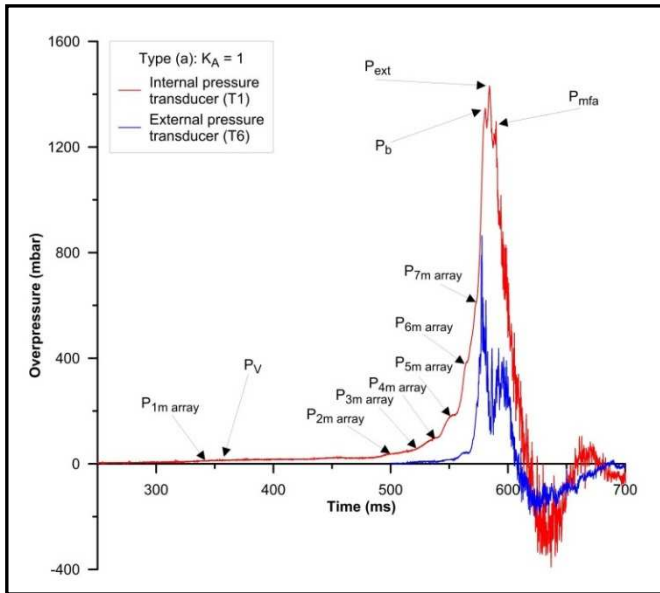


Fig. 12. Pressure-time profile for type (a) explosion, $K_A = 1$.

The P_V pressure peak has a magnitude of 18 mbar and occurred at approximately 355 ms, a similar time to that of the type (j) test shown in Fig. 11. However, the pressure peak is not obvious on the pressure-time graph due to the magnitude of the maximum pressure peak. It can be seen in Fig. 12 that the influence of the onset of burnt gas venting is significantly less than that of a type (j) explosion, which has less congestion. This observation was consistent throughout the experimental programme. The flame arrival at the second and then subsequent arrays is seen as an increase in gradient on the pressure-time curve indicating that the flame front is accelerating and interacting with obstacles immediately downstream to cause further turbulence, thereby setting up a positive feedback mechanism.

A pressure-time profile for an explosion involving a type (c) obstacle configuration with a vent size of $K_A = 4$ is shown in Fig. 13. This configuration consisted of eight arrays, each containing five pipes. The first array was located 1 m from the rear of the enclosure and the pitch between arrays was set at 1 m. However, the arrays were offset (see Fig. 2) such that the horizontal distance between each individual pipe was 2 m. The maximum overpressure generated in this explosion was 2.15 bar, considerably more than that generated in explosions with more congestion but with larger vent openings. Clearly, the generation of pressure is a combination of flame acceleration due to congestion and the degree of confinement, and it may be concluded that both congestion and confinement (i.e. less inadvertent venting) will tend to increase the observed overpressures in accidental explosions in buildings. Interestingly, with this type of configuration and vent size, the external explosion is of less influence, for the reasons described in section 4.2.1. There is a noticeable pressure differential from the rear of the chamber to the vent opening in tests involving the larger vent sizes, which is not apparent with tests of vent size $K=9$.

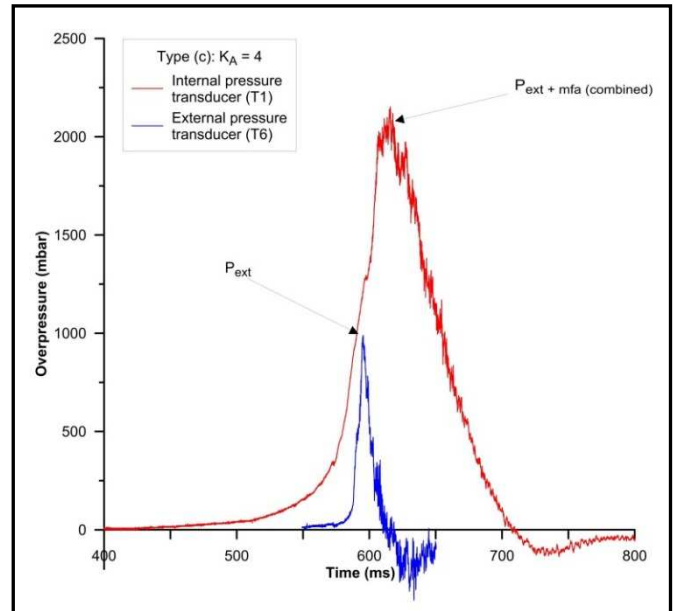


Fig. 13. Pressure-time profile for type (c) explosion, $K_A = 4$.

The effect of volume blockage on internal explosion overpressures is shown in Fig. 14 and Fig. 15. It can be seen that, in general terms, with the vent size remaining constant, the observed maximum overpressures increased as the volume blockage was increased and the maximum pressure peak occurred earlier in the explosion. This is to be expected as explosion overpressures increase with flame speed and an increasing level of congestion resulted in a higher flame speed for a given vent size (see Fig. 16). In addition, the effect of decreasing the vent size (higher vent coefficient) is to increase the overpressure because it reduces the venting rate.

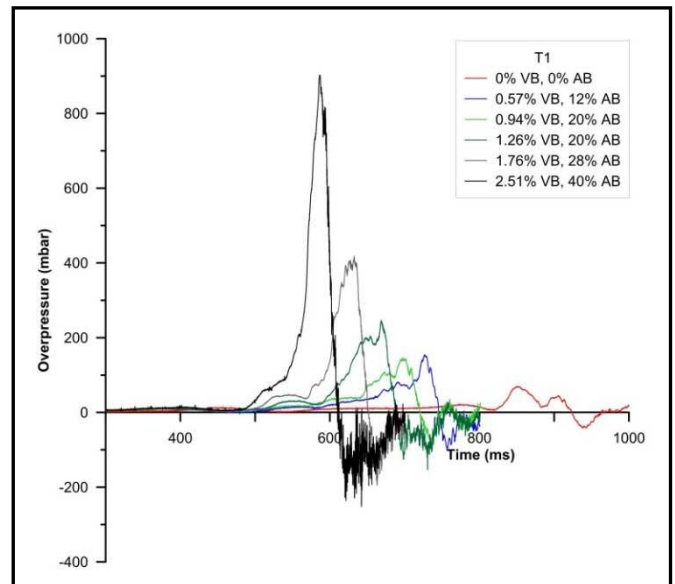


Fig. 14. The effect of volume blockage on overpressure, $K_A = 1$.

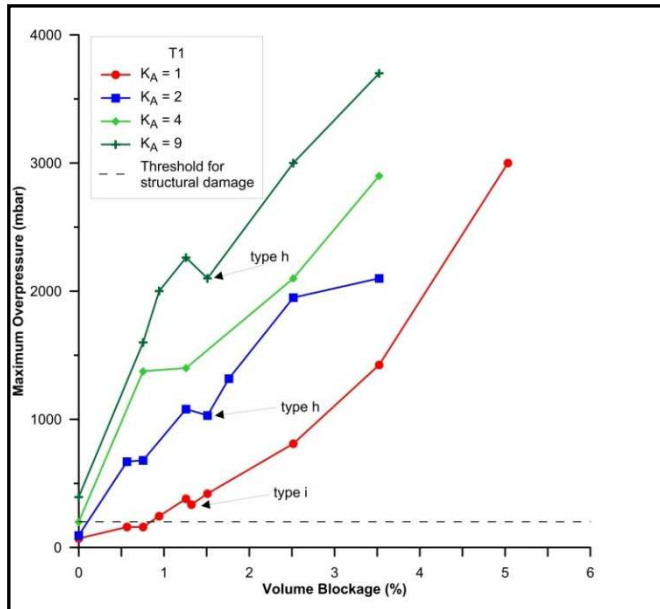


Fig. 15. The effect of volume blockage on maximum overpressure.

For any given congestion level, reducing the vent size always resulted in an increased pressure. There was therefore no point in this study where the increased flow and turbulence from the larger vent actually compensated for the effects of reducing the confinement. The noticeable reduction in overpressure observable in Fig. 15 occurs with the type (i) and type (h) congestion configurations. The type (i) configuration has three arrays and a 3.0 m pitch and the type (h) configuration has a reduced area blockage. It is therefore apparent that the area blockage and pitch play an important role in the development of fast flames and overpressure.

Interestingly, increasing the level of congestion affects the influence of the vent size on overpressure. In section 4.2.1, it was observed that reducing the vent size, for experiments with no congestion, gave rise to overpressures for $K_A = 9$ that were twice that of the corresponding value for $K_A = 4$, four times that of $K_A = 2$ and five times that of $K_A = 1$.

Table 3 shows the comparison with experiments involving congestion.

Table 3. Effects of congestion and vent size on overpressure.

Test Type	Max Pressure (bar)				Maximum Pressure Ratio					
	Vent Coefficient (K_A)				$\left(\frac{K_A = 9}{K_A = 4}\right)$	$\left(\frac{K_A = 9}{K_A = 2}\right)$	$\left(\frac{K_A = 9}{K_A = 1}\right)$	$\left(\frac{K_A = 4}{K_A = 2}\right)$	$\left(\frac{K_A = 4}{K_A = 1}\right)$	$\left(\frac{K_A = 2}{K_A = 1}\right)$
	1	2	4	9						
0% VB	0.07	0.09	0.18	0.35	1.9	3.9	5.0	2.0	2.6	1.3
m	0.16	0.67			-	-	-	-	-	4.2
l	0.16	0.68	1.37	1.6	1.2	2.4	10.0	2.0	8.6	4.3
k	0.15			2.01	-	-	13.4	-	-	-
j	0.25	1.08	1.4	2.26	1.6	2.1	9.0	1.3	5.6	4.3
h	0.34	1.04		2.1	-	2.0	6.2	-	-	3.1
e	0.42	1.28			-	-	-	-	-	3.0
c	0.72	1.94	2.15	3	1.4	1.5	4.2	1.1	3.0	2.7
d	0.9	1.98	2.92		-	-	-	1.5	3.2	2.2
b	1.43	2.27		3.7	-	1.6	2.6	-	-	1.6

It can be seen that for all tests, excluding $K_A = 1$, the addition of congestion reduces the influence of the vent size when compared to experiments without congestion. However, when comparing tests involving $K_A = 1$, the opposite is found to occur for the lower levels of congestion; with the magnitude of overpressure for a type (k) test with a vent size of $K_A = 9$, over thirteen times greater than the comparative test with $K_A = 1$, indicating that the level of congestion is insufficient to compensate for the reduction in confinement.. This is not surprising as the pressure developed within an enclosure during a vented explosion is a balance between the rate at which expanding combustion products are produced and the rate of outflow through the vent opening. Consequently, any restriction in outflow through a reduction in vent size will result in higher overpressures within the enclosure; the effect of which will be enhanced if the congestion is increased. This effect is further highlighted in

Fig. 16, where the effect of vent size on maximum overpressure is plotted. In Fig. 15 and Fig. 16, a line is plotted to indicate the pressure threshold for structural damage. It can be seen that tests without congestion ($K_A > 4$) and tests involving congestion below the levels typically found in buildings developed overpressures greater than that for structural damage for a typical building. This may suggest that most buildings involved in gas explosions would suffer significant damage. However in practice, this is not the case, as the flammable gas/air mixture is often ignited at non-stoichiometric conditions (e.g. a permanent source of ignition ignited the mixture as soon as it became flammable) such that lower flame speeds are developed, allowing more time for openings to vent and constrain the overpressure developed.

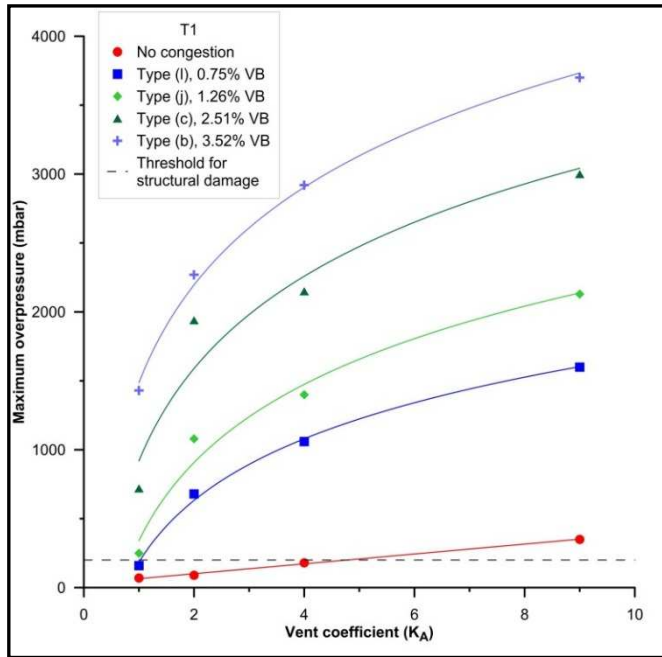


Fig. 16. The effect of vent size on maximum overpressure.

The effect of volume blockage on flame speed is shown in Fig. 17 for explosion tests where the pitch was set at 2.0 m. It can be seen that the flame speed rises as the volume blockage within the enclosure is increased, irrespective of vent size.

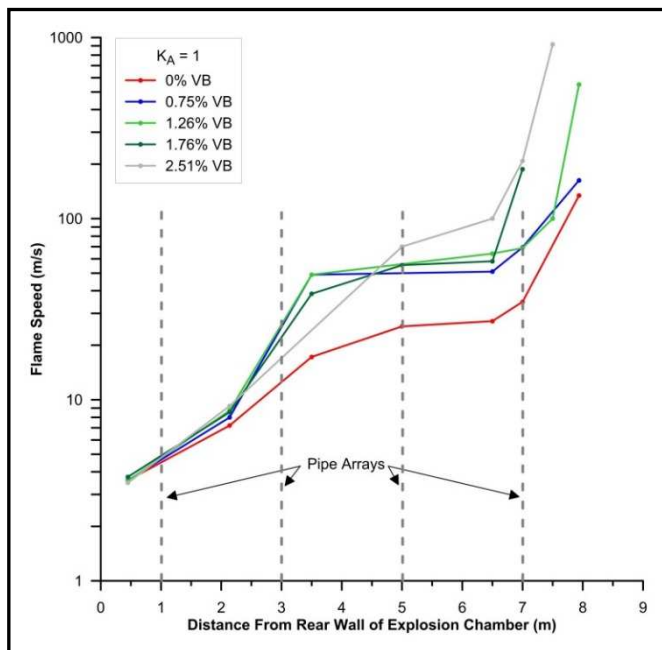


Fig. 17. Flame speed v blockage ratio.

4.3.2 Effect of Area Blockage and Pitch

The effects of the obstacle array separation distance (pitch) has received little systematic study in the literature (Na'inna, Phylaktou, & Andrews, 2014). In turbulent explosions, the maximum burning rate, and therefore the highest rate of pressure generation for a given vent size, will occur at the position of maximum turbulence intensity. It has been shown (Baines & Peterson, 1951; Na'inna et al., 2014), that the turbulence intensity increases downstream of an obstacle array until it reaches a maximum value some distance after it, and it then begins to decay at an approximately steady rate over a relatively long distance. Consequently, if a flame front

is propagating towards a series of obstacle arrays, the maximum flame speed, and hence overpressure, might be generated if the arrays were separated by the 'critical' distance; that is, each successive array is located just downstream of the position of maximum turbulence intensity, so that it receives the flame front at its peak speed, and thereby, it generates the maximum possible turbulence intensity downstream, so that the peak flame speed is received by the next obstacle, and so on. If the pitch of a series of arrays is too large or too small, then the downstream array would not be affected by the peak turbulence generated from the upstream array, resulting in an explosion of lesser severity.

During this experimental programme, a number of experiments were undertaken where the pitch and/or the area blockage was altered. However, no experiments were undertaken where the volume blockage and area blockage were constant and the pitch was altered. However, as some of the results were interesting, a brief description is detailed in this section.

A few experiments were undertaken where the area blockage and vent size were constant and the volume blockage was altered by varying the separation distance between arrays. In Fig. 18, the effect of pitch on overpressure is shown for tests where the area blockage was 20%, the vent size was $K_A = 1$ and the pitch was varied between 1.0, 2.0 and 3.0 m by altering the volume blockage. It can be seen that the greatest overpressures, and fastest flame speeds are being generated by the arrays with a pitch of 1.0 m, and the lowest overpressure is being generated where the pitch of the arrays is 3.0 m. This may simply be because the rig represents that with the largest volume blockage but further large-scale study is recommended.

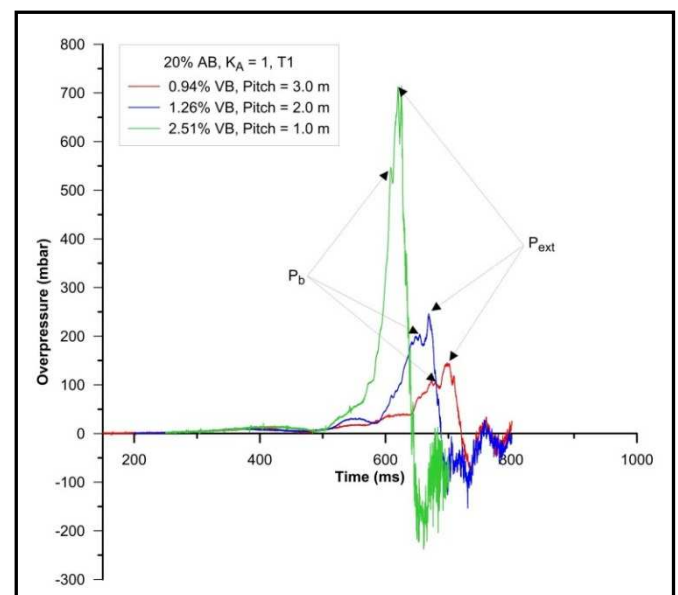


Fig. 18. The effect of pitch on overpressure.

A small number of experiments were undertaken where the volume blockage and vent size were constant and the area blockage and the separation distance between arrays was altered. The effect of area blockage and pitch on overpressure is shown in Fig. 19 for tests where the volume blockage was 2.51%, the vent size was $K_A = 1$ and the pitch was varied between 1.0 and 2.0 m. It can be seen that the greatest overpressures and fastest flame speeds are generated when

the area blockage was greatest. Further large-scale studies into the effect of area blockage is recommended.

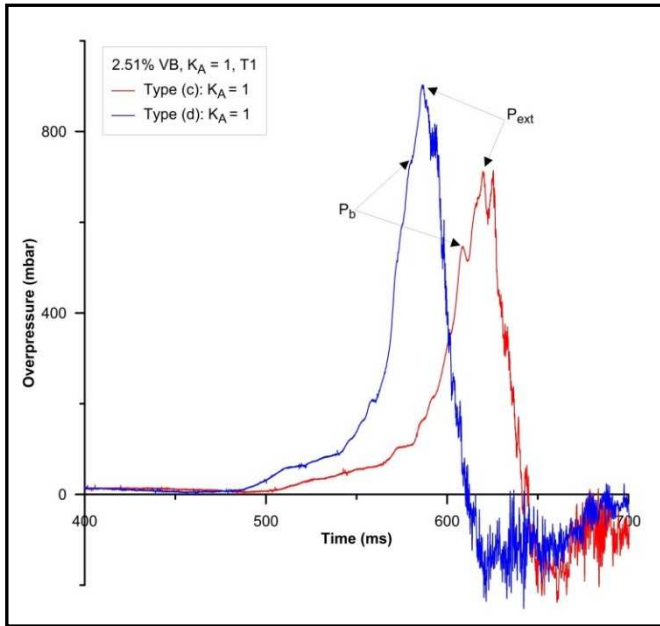


Fig. 19. The effect of area blockage and pitch on overpressure.

5 CONCLUSIONS

The series of tests produced peak explosion overpressures of between 70 mbar ($K_A = 1$ and no congestion) to 3.7 bar ($K_A = 9$ and 3.52% VB) with corresponding maximum flame speeds in the range 35 - 395 m/s at a distance of 7 m from the ignition point. Flame speeds in excess of 600 m/s were consistently recorded close to the vent opening during tests with area blockages of 20% or greater combined with a volume blockage greater than 1.5%. One test configuration (Type (a)), was only utilised for tests with a vent opening of $K_A = 1$, as the overpressures predicted for tests involving a vent opening of $K_A = 2, 4$ or 9, based on earlier experiments, exceeded the design strength of the explosion chamber.

The results of these large-scale experiments show that high and damaging overpressures can be generated even from explosions in empty (no internal congestion) enclosures if the vent opening is such that it prevents sufficient outflow. The presence of congestion was found to significantly increase the overpressures generated, often by more than an order of magnitude. The tests demonstrated that it was possible to generate overpressures capable of causing structural damage in empty chambers if the vent openings do not allow sufficient outflow. Furthermore, with volume blockages of as little as 0.57%, overpressures greater than 200 mbar were generated in all tests where $K_A > 1$. They also confirmed that reducing the vent size always increased the overpressure regardless of the degree of congestion. The significance of these results is that they confirm that the size and failure pressure of potential vent openings, and the degree of congestion within a building, are key factors in whether or not a building will sustain structural damage following a gas explosion. Given that the average volume blockage in a room in a UK dwelling is in the order of 17%, it is clear that without the use of large windows of low failure pressure, buildings will continue to be susceptible to significant structural damage during an accidental gas explosion.

NOMENCLATURE

- A the area of the front face of the explosion chamber, m^2
- A_{cs} the cross sectional area of the explosion chamber, m^2
- A_v the area of the vent opening, m^2
- AB percentage of the cross-sectional area of the explosion chamber occupied by the pipes in a single idealised pipe array, %
- K_A ($K_A = A/A_v$),
- L/D length to diameter ratio, -
- P_b overpressure peak at which the onset of burnt gas venting occurs, mbar
- P_{ext} overpressure peak at which the external explosion occurs, mbar
- P_{max} maximum overpressure, mbar
- P_{mfa} overpressure peak at the time of maximum flame area, mbar
- P_v overpressure peak at the time the vent opens, mbar
- type (a) idealised congested region comprising eight arrays of 10 x 180 mm pipes, positioned with a 1 m pitch, giving an area blockage of 40% and a volume blockage of 5.02%
- type (b) idealised congested region comprising eight arrays of 7 x 180 mm pipes, positioned with a 1 m pitch, giving an area blockage of 28% and a volume blockage of 3.52%
- type (c) idealised congested region comprising eight arrays of 5 x 180 mm pipes, positioned with a 1 m pitch, giving an area blockage of 20% and a volume blockage of 2.51%
- type (d) idealised congested region comprising four arrays of 10 x 180 mm pipes, positioned with a 2 m pitch, giving an area blockage of 40% and a volume blockage of 2.51%
- type (e) idealised congested region comprising four arrays of 7 x 180 mm pipes, positioned with a 2 m pitch, giving an area blockage of 28% and a volume blockage of 1.76%
- type (f) idealised congested region comprising four arrays of 7 x 180 mm pipes, positioned in the 1st half of the explosion chamber, with a 1 m pitch, giving an area blockage of 28% and a volume blockage of 1.76%
- type (g) idealised congested region comprising four arrays of 7 x 180 mm pipes, positioned in the 2nd half of the explosion chamber, with a 1 m pitch, giving an area blockage of 28% and a volume blockage of 1.76%
- type (h) idealised congested region comprising eight arrays of 3 x 180 mm pipes, positioned with a 1 m pitch, giving an area blockage of 12% and a volume blockage of 1.51%

- type (i) idealised congested region comprising three arrays of 7 x 180 mm pipes, positioned with a varied pitch, giving an area blockage of 28% and a volume blockage of 1.31%
- type (j) idealised congested region comprising four arrays of 5 x 180 mm pipes, positioned with a 2 m pitch, giving an area blockage of 20% and a volume blockage of 1.26%
- type (k) idealised congested region comprising three arrays of 5 x 180 mm pipes, positioned with a varied pitch, giving an area blockage of 20% and a volume blockage of 0.94%
- type (l) idealised congested region comprising four arrays of 3 x 180 mm pipes, positioned with a 2 m pitch, giving an area blockage of 12% and a volume blockage of 0.75%
- type (m) idealised congested region comprising three arrays of 3 x 180 mm pipes, positioned with a varied pitch, giving an area blockage of 12% and a volume blockage of 0.57%
- V volume of the explosion chamber, m³
- VB percentage of the total volume of the explosion chamber occupied by the pipes in all idealised pipe arrays, %

REFERENCES

- Admirals Storage. How much space do I need. 2015, from <http://www.admiralstorage.co.uk/how%20much%20space.html>
- Alexiou, A., Andrews, G., & Phylaktou, H. (1997). A Comparison between End-Vented and Side-Vented Gas Explosions in Large L/D Vessels. *Process Safety and Environmental Protection*, 75(1), 9-13. doi: 10.1205/095758297528715
- Alexiou, A., Andrews, G. E., & Phylaktou, H. (1996). Side-vented gas explosions in a long vessel: the effect of vent position. *Journal of Loss Prevention in the Process Industries*, 9(5), 351-356. doi: 10.1016/0950-4230(96)00029-0
- Alexiou, A., Phylaktou, H., & Andrews, G. E. (1996). The Effect of Vent Size on Pressure Generation in Explosions in Large L/D Vessels. *Combustion Science and Technology*, 113(1), 645 - 652.
- Astbury, N. F., & Vaughan, G. N. (1972). Motion of Brickwork Structure Under Certain Assumed Conditions: The British Ceramic Research Association.
- Astbury, N. F., West, H. W. H., Hodgkinson, H. R., Cabbage, P. A., & Clare, R. (1970). Gas Explosions in Load-Bearing Brick Structures: The British Ceramic Research Association.
- Baines, W. D., & Peterson, E. G. (1951). Investigation of flow through screens. *American Society of Mechanical Engineers - Transactions*, 73(5), 467-477.
- Baker, W. E., Cox, P. A., Kulesz, J. J., Strehlow, R. A., & Westine, P. S. (1983). *Explosion Hazards and Evaluation*: Elsevier Science.
- Bauwens, C. R., Chaffee, J., & Dorofeev, S. (2010). Effect of Ignition Location, Vent Size, and Obstacles on Vented Explosion Overpressures in Propane-Air Mixtures. *Combustion Science and Technology*, 182(11), 1915 - 1932.
- Bauwens, C. R., Chaffee, J. L., & Dorofeev, S. (2009). *Experimental and Numerical Study of Methane-air Deflagrations in a Vented Enclosure*. Paper presented at the Ninth International Symposium on Fire Safety Science.
- BBC news (Producer). (2011). 'Shoobox homes' become the UK norm. Retrieved from <http://www.bbc.co.uk/news/uk-14916580>
- Bimson, S. J., Bull, D. C., Cresswell, T. M., Marks, P. R., Masters, A. P., Prothero, A., . . . Samuels, B. (1993). *An experimental study of the physics of gaseous deflagration in a very large vented enclosure*. Paper presented at the 14th International Colloquium on the Dynamics of Explosions and Reactive Systems, , Coimbra, Portugal.
- Chan, C., Moen, I. O., & Lee, J. H. S. (1983). Influence of confinement on flame acceleration due to repeated obstacles. *Combustion and Flame*, 49(1-3), 27-39. doi: 10.1016/0010-2180(83)90148-7
- Cooper, M. G., Fairweather, M., & Tite, J. P. (1986). On the mechanisms of pressure generation in vented explosions. *Combustion and Flame*, 65(1), 1-14. doi: [http://dx.doi.org/10.1016/0010-2180\(86\)90067-2](http://dx.doi.org/10.1016/0010-2180(86)90067-2)
- Drury, A., Watson, J., Broomfield, R., Levitt, D., & Tetlow, R. (2006). Housing Space Standards (Mayor of London, Trans.): HATC Ltd.
- Eckhoff, R. K., Fuhre, K., Guirao, C. M., & Lee, J. H. S. (1984). Venting of turbulent gas explosions in a 50 m³ chamber. *Fire Safety Journal*, 7(2), 191-197. doi: [http://dx.doi.org/10.1016/0379-7112\(84\)90039-0](http://dx.doi.org/10.1016/0379-7112(84)90039-0)
- Fakandu, B. M. (2014). *Vented Gas Explosions*. (PhD PhD), University of Leeds.
- Fakandu, B. M., Andrews, G. E., & Phylaktou, H. N. (2014, 10-14 June). *Impact of non-central vents on vented explosion overpressures*. Paper presented at the Tenth International Symposium on Hazards, Prevention, and Mitigation of Industrial Explosions (X ISHPMIE), Bergen, Norway.
- Fakandu, B. M., Kasmani, R. M., Andrews, G. E., & Phylaktou, H. N. (2011). *Explosion Venting and Mixture Reactivity Influences in a Small Vessel*. Paper presented at the 23rd ICDERS, University of California, Irvine.
- Fakandu, B. M., Yan, Z. X., Phylaktou, H. N., & Andrews, G. E. (2013, May 5-10). *The Effect of Vent Area Distribution in Gas Explosion Venting and Turbulent Length Scale Influence on the External Explosion Overpressure*. Paper presented at the Seventh International Seminar on Fire & Explosion Hazards (ISFEH7), Providence, Rhode Island.
- Greater London Authority. (2012). Housing: supplementary planning guidance (Mayor of London, Trans.).
- Hall, R., Masri, A., Yaroshchuk, P., & Ibrahim, S. (2009). Effects of position and frequency of obstacles on turbulent premixed propagating flames. *Combustion and Flame*, 156(2), 439-446. doi: 10.1016/j.combustflame.2008.08.002
- Harris, R. J. (1983). *The Investigation and Control of Gas Explosions and Heating Plant*. London: E & F Spon Ltd.
- Harris, R. J., & Wickens, M. J. (1989). Understanding vapour cloud explosions - an experimental study. *IGE Communication 1408*.
- Harrison, A. J., & Eyre, J. A. (1987). External Explosions as a Result of Explosion Venting. *Combustion Science and Technology*, 52(1), 91 - 106.
- Mercx, W. P. M., van Wingerden, C. J. M., & Pasman, H. J. (1993). Venting of gaseous explosions. *Process Safety Progress*, 12(1), 40-46. doi: 10.1002/prs.680120106
- Na'inna, A. M., Phylaktou, H. N., & Andrews, G. E. (2013a). The acceleration of flames in tube explosions with two

- obstacles as a function of the obstacle separation distance. *Journal of Loss Prevention in the Process Industries*, 26(6), 1597-1603. doi: <http://dx.doi.org/10.1016/j.jlp.2013.08.003>
- Na'inna, A. M., Phylaktou, H. N., & Andrews, G. E. (2013b). *Acceleration of Flames in Tube Explosions with Two Obstacles as a Function of the Obstacle Separation Distance: The Influence of Mixture Reactivity*. Paper presented at the Proc. of the Seventh International Seminar on Fire & explosion Hazards (ISFEH7), Providence, USA.
- Na'inna, A. M., Phylaktou, H. N., & Andrews, G. E. (2014). Effects of Obstacle Separation Distance on Gas Explosions: The Influence of Obstacle Blockage Ratio. *Procedia Engineering*, 84(0), 306-319. doi: <http://dx.doi.org/10.1016/j.proeng.2014.10.439>
- Pappas, J. A. (1983). *Gas Explosions: Venting of Large Scale Volumes*. Paper presented at the International Symposium Organised by Oyez Scientific and Technical Services Ltd.
- Pappas, J. A., Solberg, D. M., & Foyn, T. E. (1984). Final Report *Gas Explosion Research Programme*: Det Norske Veritas.
- Park, D. J., Lee, Y. S., & Green, A. R. (2008). Experiments on the effects of multiple obstacles in vented explosion chambers. *Journal of Hazardous Materials*, 153(1-2), 340-350. doi: <http://dx.doi.org/10.1016/j.jhazmat.2007.08.055>
- Phylaktou, H., Alexiou, A., & Andrews, G. (1995). Interaction of Fast Explosions with an Obstacle: Health and Safety Executive.
- Phylaktou, H., & Andrews, G. E. (1994). Prediction of the maximum turbulence intensities generated by grid-plate obstacles in explosion-induced flows. *Symposium (International) on Combustion*, 25(1), 103-110. doi: [http://dx.doi.org/10.1016/S0082-0784\(06\)80634-X](http://dx.doi.org/10.1016/S0082-0784(06)80634-X)
- Phylaktou, H. N. (1993). *Gas Explosions in Long Closed Vessels with Obstacles: A turbulent combustion study applicable to industrial explosions*. (PhD), University of Leeds.
- Pritchard, D. K., Hedley, D., & Webber, N. K. (2002). Effect of Obstacles on Flame Acceleration and Explosion Development: HSL.
- Solberg, D. M., Pappas, J. A., & Skramstad, E. (1980). *Experimental investigations on flame acceleration and pressure rise phenomena in large scale vented gas explosions*. Paper presented at the 3rd International Symposium on Loss Prevention and Safety Promotion in the Process Industries., Basle, Switz.
- Taylor, P. H., & Bimson, S. J. (1989). Flame propagation along a vented duct containing grids. *Symposium (International) on Combustion*, 22(1), 1355-1362. doi: [http://dx.doi.org/10.1016/S0082-0784\(89\)80146-8](http://dx.doi.org/10.1016/S0082-0784(89)80146-8)
- van Wingerden, C. J. M. (1984a). An Experimental Study into the Venting of Gaseous Explosions: Part 1 - Experimental Results: TNO.
- van Wingerden, C. J. M. (1984c). Experimental Study of the Influence of Obstacles and Partial Confinement on Flame Propagation: Commission of the European Communities for nuclear science and technology.
- van Wingerden, C. J. M. (1989). *On the venting of large-scale methane-air explosions*. Paper presented at the Sixth international symposium of loss prevention and safety promotion in the process industries, Oslo.
- van Wingerden, C. J. M., & Zeeuwen, J. P. (1983a). Flame propagation in the presence of repeated obstacles: Influence of gas reactivity and degree of confinement. *Journal of Hazardous Materials*, 8(2), 139-156. doi: 10.1016/0304-3894(83)80053-3
- van Wingerden, C. J. M., & Zeeuwen, J. P. (1983c). *Venting of gas explosions in large rooms*. Paper presented at the 4th International Symposium on Loss Prevention and Safety Promotion in the Process Industries (EFCE Event n 290). Volume 3: Chemical Process Hazards., Harrogate, England.
- West, H. W. H., Hodgkinson, H. R., & Webb, W. F. (1971a). The Resistance of Brick Walls to Lateral Loading (pp. 141 - 178): The British Ceramic Research Association.
- West, H. W. H., Hodgkinson, H. R., & Webb, W. F. (1971b). The Resistance of Clay Brick Walls to Lateral Loading: The British Ceramic Research Association.
- Wong, C. W., & Karamanoglu, M. (1999). Modelling the response of masonry structures to gas explosions. *Journal of Loss Prevention in the Process Industries*, 12(3), 199-205. doi: [http://dx.doi.org/10.1016/S0950-4230\(98\)00058-8](http://dx.doi.org/10.1016/S0950-4230(98)00058-8)
- Zalosh, R. G. (1980). *Gas explosion tests in room-size vented enclosures*. Paper presented at the AIChE Loss Prevention Symposium, Houston, TX, USA.
- Zalosh, R. G. (2008). Explosion Venting Data and Modeling Research Project: Fire Protection Research Foundation.